Excited states of tetrahedral single-core Si_{29} nanoparticles

S. Rao, J. Sutin, R. Clegg, E. Gratton, and M. H. Nayfeh*
Department of Physics, University of Illinois at Urbana-Champaign, 1110 West Green Street, Urbana, Illinois 61801, USA

S. Habbal
Institute of Mathematical and Physical Sciences, The University of Wales at Aberystwyth, Ceridigion SY23 3BZ, United Kingdom

A. Tsolakidis and R. M. Martin
Department of Physics and Materials Research Laboratory, University of Illinois at Urbana-Champaign, 1110 West Green Street, Urbana, Illinois 61801, USA

(Received 7 November 2003; published 28 May 2004)

We dispersed bulk crystalline Si into identical hydrogenated nanoparticles with negligible impurities and defects, which provide the opportunity for detailed comparison between measurement and theory. The UV photoluminescence of a dispersion of 1 nm silicon particles was studied. Distinct bands appear in the emission spectra with the lowest peaks in wavelength identified to be at 400, 360, and 310 nm with optimal excitation at 3.7, 4.0, and 4.6 eV, respectively. The multiple photoluminescence bands are analyzed in terms of the molecularlike energy levels of one bulklike and two nonbulklike reconstruction configurations of the filled fullerene single-core $Si_{29}H_{24}$, calculated by quantum Monte Carlo calculations and by time-dependent density functional theory. The measured bands are in close agreement with the excited states of the ideal bulklike configuration. However, there is a possibility that some of the observed bands might originate from the nonbulklike reconstructions. The Stokes shifts are discussed in terms of radiative relaxation via the molecularlike states versus charge carrier relaxation via the underlying continuum states.

DOI: 10.1103/PhysRevB.69.205319 PACS number(s): 73.22.−f, 78.67.Bf

INTRODUCTION

Semiconductor clusters, especially silicon, comprise one of the most active frontiers in physics, chemistry, and biophysics. Studies have focused on their unique structures, stability, and chemical reactivity and on their optical, electronic, and functional properties. The optical characteristics of Si nanostructures were mostly studied using porous silicon samples.[1–5] Quantum confinement of charge carriers, intrinsic radiative surface sites, extrinsic radiative defects, or extrinsic chemical species related to silicon oxygen compounds are among the models that have been discussed over the last several years. However, the analysis is not straightforward because porous Si consists of interconnected wirelike structures of random size, shape, and chemical composition, with nanostructures being mostly larger than 2–3 nm. Analysis performed under heavy statistical averaging makes it hard to differentiate between theoretical models. Despite significant progress toward elucidation of the structure and the mechanism responsible for the visible photoluminescence or optical characteristics in general, the problem of the strong optical activity of Si nanostructures remains open.

There has not been an *a priori* way for selective excitation or enriching a particular distribution of crystallite sizes and shapes in porous Si. A reproducible method to create fluorescent Si nanoparticles with a high control over their size, shape, and orientation would alleviate these problems and allow straightforward measurements and interpretation. Recently, we developed an electrochemical etching method for dispersion of bulk crystalline Si into identical hydrogenated nanoparticles with negligible defects,[6–12] which provides the opportunity for detailed comparison between measurement and theory. We produced samples consisting of discrete sizes in the range of 1–3 nm. Discrete sizes in this range are very valuable since they exhibit strong distinct photoluminescence in the red, green, and blue (RGB), useful for biomedical tagging and in RGB display applications.[6] The smallest particles (1 nm in diameter) are ultrabright blue luminescent such that emission from single particles is readily detectable.[7] The emission from aggregates of the particles exhibits highly nonlinear stimulated emission,[8] collimated blue and red laser beam emission,[9,10] and second harmonic generation.[11] The particle's capacitance is small so that the single electron charging energy or the quantum confinement electronic energies are larger than the thermal agitation, allowing single electronics at room temperature.[12]

The 1 nm Si nanoclusters are amenable to testing and accurate first-principles simulations because they consist of a manageable number of Si and H atoms and are produced in macroscopic amounts. Thus, these particles have been attracting experimental[6–12] and theoretical[13–19] attention. Calculations based upon density functional theory with a generalized gradient exchange-correlation potential, configuration interaction, and Monte Carlo approaches suggest a filled fullerene structure for $Si_{29}H_{24}$ (1 nm).[15–17] The molecular structure of this hydrogenated configuration was calculated for several specific surface reconstructions, from fully constructed to nonconstructed surfaces.[15–19] The structure, shown in Fig. 1(a),[15–17] referred to as ideal bulklike, is nearly spherical but contains a combination of hexagon and pentagon ring structures (T_d point group symmetry) that produce a highly wrinkled or ''puckered-ball'' surface. It consists of a central core Si atom and four Si atoms in a tetrahedral coordination, constituting an inner core (inner shell). The remain-

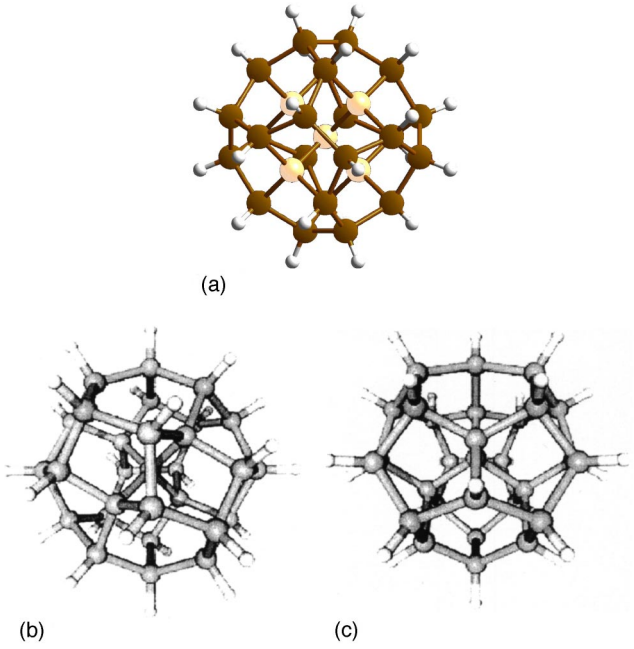

FIG. 1. Structural prototypes of a particle that contains 29 silicon atoms (magic number for the T_d symmetry and spherical shape). (a) Bulklike (light atoms are the Si atoms that make up the inner core). Small white (hydrogen), large dark (hydrogenated silicon), and large light (silicon). (b) $Si_{29}H_{24}^{nano1}$. (c) $Si_{29}H_{24}^{nano2}$. Small white (hydrogen) and large dark (silicon). The two configurations (b) and (c) essentially feature two other ways to connect the inner T_d Si atom to the surface, while keeping all of the hydrogen on the surface.

ing 24 atoms constitute an outer Si surface (outer shell), which has a hydrogen-terminated bulklike (2×1) reconstruction of dimer pairs on (001) facets (six reconstructed surface dimers). Alternatively, one can think of the structure as a 28-atom fullerene cage with a T_d atom in the center. Once the core atom is connected to the fullerene, the remaining atoms are passivated with hydrogen. Quantum Monte Carlo simulations[15] yield a size of 0.9 nm, band gap of 3.5 $\pm$0.1 eV, and Stokes shift of 0.4 eV with an emission band in the blue under 355 nm excitation. In addition to the ideal bulklike construction described above, there is a recent proposal[18] of two other unique ways to connect the interior core atom to the surface and maintain a tetrahedral core. This results in two different configurations, $Si_{29}H_{24}^{nano1}$ and $Si_{29}H_{24}^{nano2}$, shown in Figs. 1(b) and 1(c),[18] that have no full bulk analog. The three $Si_{29}H_{24}$ configurations are of the same size and contain hydrogen only at the surface. The nonbulklike configurations, however, have surfaces that differ from the bulklike reconstruction that resulted in the six reconstructed surface dimer pairs. They also exhibit larger quantum Monte Carlo (QMC) band gaps, namely, 4.5 and 4.1 eV for $Si_{29}H_{24}^{nano1}$ and $Si_{29}H_{24}^{nano2}$, respectively,[18] compared to 3.5 eV for the bulklike configuration.

In this paper, the intrinsic molecularlike structure and photoluminescence bands of the 1 nm particle are studied by mapping out the excitation and emission bands of a suspension of the nanoparticles. In addition to the known blue luminescence at 400 nm with a band gap of 3.7 eV, the results identify two more emission bands. The bands lie in the UV and peak at 310 and 360 nm, with optimal excitation energies of 4.0 and 4.6 eV. In order to compare with theory, the calculations of the molecularlike excited states of the ideal bulklike construction of the $Si_{29}H_{24}$ prototype configuration and the two nonbulklike configurations of $Si_{29}H_{24}$ using time-dependent density functional theory (TDDFT) are presented. The results of these TDDFT calculations indicate that the experimentally measured absorption peaks of 3.7, 4.0, and 4.6 eV are present not only in the optical spectrum of the bulklike reconstruction of $Si_{29}H_{24}$ but in the two nonbulklike configurations as well.

EXPERIMENT

The samples originate from crystalline Si that is dispersed into nanoparticles through electrochemical etching with HF and H_2O_2.[6–12,20] The wafer is laterally anodized while slowly being advanced into the acid bath to produce a large meniscuslike area. The combination of HF and H_2O_2 takes advantage of the highly reactive nature of HF with silicon oxide, resulting in the production of smaller particles. In addition, the oxidative and cleansing nature of the peroxides produces chemically and electronically high-quality samples.[20] The pulverized wafer is then transferred to an ultrasound bath for a brief treatment, under which the film crumbles into a colloidal suspension of blue-emitting particles. High-resolution transmission electron microscope imaging shows that the particles are nearly spherical and approximately 1.0 nm in diameter.[20]

The excitation spectrum, i.e., the absorption monitored at a specific emission wavelength (product of absorption and emission quantum efficiency) was recorded on a photon counting spectrofluorometer with a Xe arc lamp light source and 4 nm bandpass excitation and emission monochrometers. The excitation wavelength was varied between 250 and 400 nm, while collecting the emission in the range 250–600 nm at each excitation wavelength. The result, a ''matrix'' of data from varying both wavelengths with a small step size, allows for analysis of both emission characteristics at different excitation wavelengths and optimal excitation wavelengths for fixed emission wavelengths. Selected emission spectra from one of the samples are shown in Figs. 2(a)–2(j), with each spectrum originating from a different excitation wavelength. Thus, the figure shows how the emission changes as the excitation wavelength is walked from 250 to 400 nm. Distinct emission bands are observed, centered at 310, 360, and 390 nm. The corresponding excitation bands for these emission wavelengths are centered at 275, 310, and 335 nm (4.6, 4.0, and 3.7 eV), respectively. For both the emission and excitation, the bands are fairly broad with widths $\sim$40–70 nm. At the optimal yield of the resonance, the relative brightness (product of absorption and quantum efficiency) of the emission bands is calculated roughly to be 7:2:1, with peak-to-peak Stokes shifts of 0.51, 0.56, and 0.53 eV, respectively. We also observe an emission band at 440 nm (2.8 eV) that overlaps with the 390 nm band, with a 410 nm center of weight for the combined bands.

Density functional theory with generalized gradient

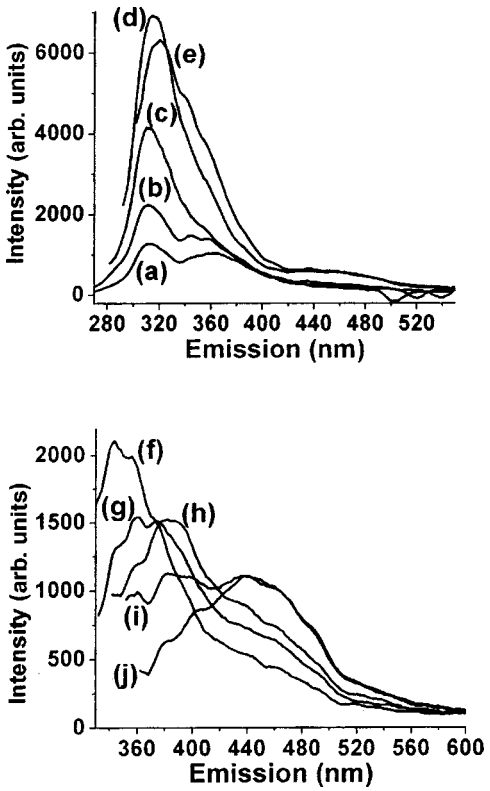

FIG. 2. A series of emission line profile spectra for a typical sample with corresponding excitation wavelength: (a) 250, (b) 260, (c) 270, (d) 280, (e) 290, (f) 310, (g) 320, (h) 335, (i) 340, and (j) 350 nm. Distinct emission bands are observed centered at 310, 360, 390, and 440 nm. The curves (d), (f), (h), (j) represent the optimal response of the bands, with excitation wavelengths of 275, 310, 335, and 355 nm, respectively, or 4.5, 4.0, 3.7, and 3.5 eV. The center of weight of the overlapping band of 390 and 440 nm at 410 nm maximizes for excitation at ~3.6 eV.

exchange-correlation potential, configuration interaction, and Monte Carlo approaches yield sharply structured spectra including the transition $T1 \rightarrow T2$, which corresponds to the edge of the absorption spectrum.[15–17] The lowest few transitions occur at 3.55, 3.95, 4.55, 4.90, 5.05, 5.80, and 5.95 eV, as shown in Fig. 3, which gives the experimental absorption spectrum along with the calculated QMC results.

THEORY

We calculated the absorption spectrum of the three configurations of $Si_{29}H_{24}$ using TDDFT. Our implementation involves the description of the electronic states using linear combination of atomic orbitals. Our scheme is based on the SIESTA code,[21–23] which is used to compute the initial wave functions and the Hamiltonian matrix for each time step. Core electrons are replaced by norm-conserving pseudopotentials[24] in the fully nonlocal Kleinman-Bylander form,[25] and the basis set is a general and flexible linear combination of numerical atomic orbitals (NAOs), constructed from the eigenstates of the atomic pseudopotentials.[22,26]

The calculations are done in the time domain, explicitly evolving the wave functions by solving the time-dependent

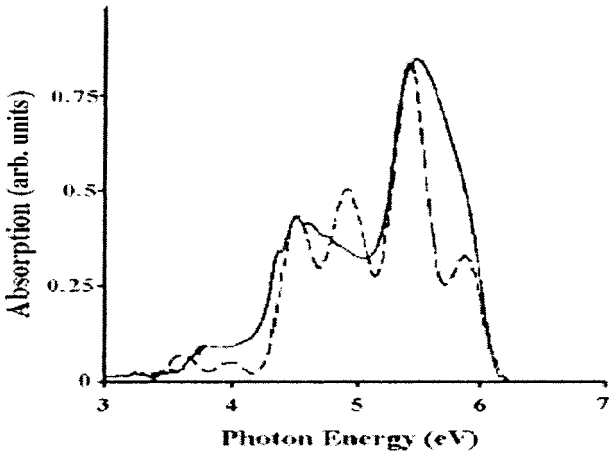

FIG. 3. The experimental absorption spectrum of the ideal bulklike configuration of a $Si_{29}H_{24}$ cluster, along with the spectrum calculated using QMC from Ref. 15.

Kohn-Sham equation. We approximate the exchange-correlation potential using the adiabatic local density approximation in which the exchange-correlation potential is local in time and space. For every time step we solve the Kohn-Sham equation using the Crank-Nicholson operator method,[27] and from the new wave functions we obtain the electron density, which is used for the calculation of the Hamiltonian in the new cycle. For calculation of the optical response, the cluster is treated as a bounded system in a finite electric field, and the ground state is found using standard time-independent density functional theory. Then we switch off the electric field at time $t=0$, and for every subsequent time step we propagate the occupied Kohn-Sham eigenstates and calculate the dipole moment. The Fourier transform of the dipole moment finally leads to the frequency-dependent polarizability tensor and average linear polarizability. The quantity of interest is the dipole strength function S; it is proportional to the photoabsorption cross section recorded in our experiments and, therefore, allows direct comparison. In addition, the integration of S over energy gives the number

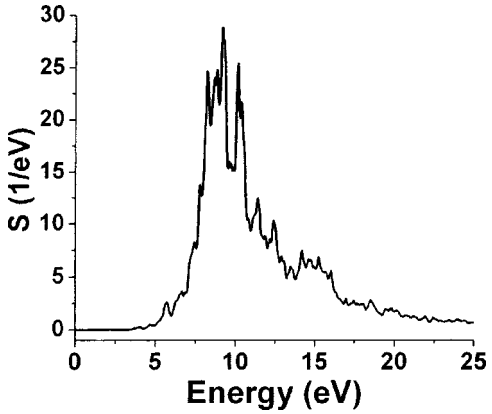

FIG. 4. The absorption spectrum of the ideal bulklike configuration of the $Si_{29}H_{24}$ cluster for the range 0–25 eV, calculated within time-dependent density functional theory using the approach of Ref. 28.

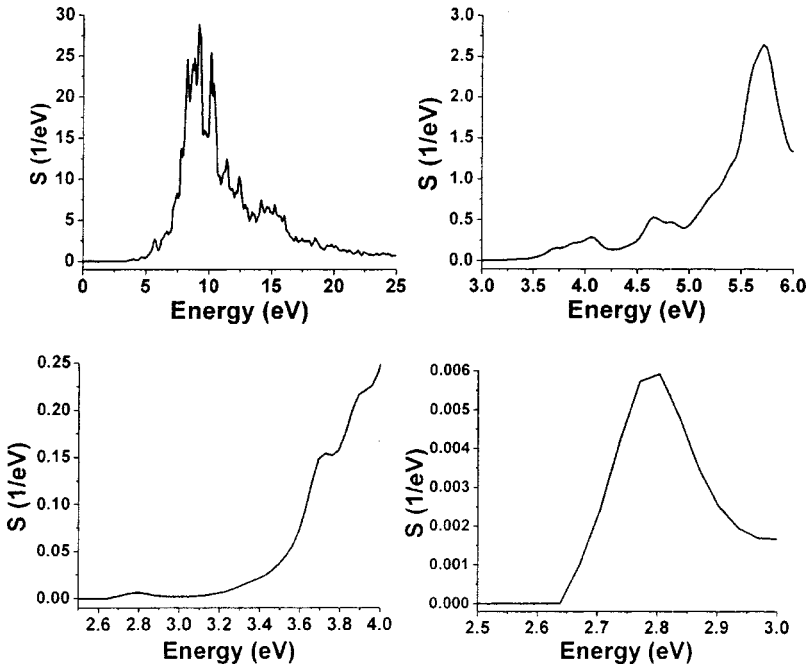

FIG. 5. The absorption spectrum of the ideal bulklike configuration of $Si_{29}H_{24}$ for different photon energy ranges.

of electrons; therefore providing a test for the quality of the calculation. More details about the theoretical method can be found in the recently published paper.[28]

Figures 4 and 5(a)–5(d) give the calculated optical spectrum of the bulklike reconstruction of $Si_{29}H_{24}$ using TDDFT for different energy ranges. In the calculation, we let the system evolve for the total time of $T=94.26\ \mathrm{eV}^{-1}$ or 389.83 fs. The energy resolution is, in consequence, equal to 0.033 eV. The time step is $7.350\times10^{-3}\ \mathrm{eV}^{-1}$, and the damping factor used in the Fourier transform is 0.095 eV. An auxiliary real-space grid[21] equivalent to a plane-wave cutoff of 70 Ry is also used in this calculation. The basis set for Si includes 25 numeric atomic orbitals per atom: two radial shapes to represent the $3s$ states with confinement radii $r_s=6.12$ a.u, two $3p$ and $3d$ shells with radii $r_p=7.85$ and $r_d=8.68$ a.u., plus an additional polarization[22] d shell with confinement radius $r_d^{\mathrm{pol}}=8.68$ a.u. The basis set for H includes five NAOs per atom: two radial shapes to represent the $1s$ states and an additional polarization s shell with radii $r_s=r_s^{\mathrm{pol}}=6.05$ a.u.

The calculations give overlapping bands centered at ~4.6, 4.0, and 3.6 eV, in fair agreement with the three bands seen in the measurements. The next higher excited bands or modulations in the absorption occur at 4.85, 5.15, and 5.75 eV. These lowest six bands are in reasonable agreement with the quantum Monte Carlo calculations of the Si_{29} configuration. The peak at 3.6 eV in the TDDFT calculation may be associated with the highest occupied–lowest unoccupied molecular orbital (HOMO-LUMO) peak observed in the QMC calculations. However, observing the low-energy absorption spectrum below 3.6 eV in the TDDFT, we notice a small peak at 2.8 eV. The fact that the oscillator strength of this peak is so small signifies that it corresponds to a ''forbidden'' transition. Because of localization effects this transition is now possible but carries little oscillator strength. The small oscillator strength has as a consequence a tiny correction in the energy from the exchange and correlation effects included in TDDFT. This is one possible explanation why the energy of the peak is close to the Kohn-Sham gap of around 2.5 eV. The emission at 440 nm (2.8 eV) observed in the measurements may be related to this band; however, the observed band may be associated with defects in the hydrogen passivation such as the presence of a single oxygen site.

Time-dependent density functional theory[29] was previously used to examine nonhydrogenated Si clusters as small as 2.5 nm diameter particles. But only the optical gap was calculated and no surface construction effects were analyzed. Linear response calculations within the time-dependent local density-functional formalism were also used to obtain the photoabsorption cross sections of very small nonhydrogenated silicon clusters (Si_4 and Si_6).[30] The TDDFT method was also used to calculate the optical absorption spectrum of hydrogenated silicon clusters in the presence of oxygen on the surface.[31] In those calculations the systems $Si_{35}H_{34}$ and $Si_{29}H_{34}$ were analyzed in the presence of oxygen on the surface (i.e., $Si_{35}OH_{34}$ and $Si_{29}OH_{34}$), in either a bridge formation (Si-O-Si) or a single double bond formation (Si═O). The calculations show that local resonance structures in the absorption at 3.5 eV and higher are introduced for a bridgelike defect and at 3.2 eV and higher for a double-bond defect. The computed spectra demonstrated that oxidation effectively reduces optical gaps in silicon clusters by as much as 1–2 eV. The effect of oxygen passivation on Si_{29}, in the configuration $Si_{29}O_6H_{24}$ was also examined using hybrid functional density functional theory.[32] The change in the size of the optical gaps was consistent with the redshift of photoluminescence observed in oxidized silicon nanocrystals (Ref. 4, for example). Although those calculations did not analyze the fully reconstructed $Si_{29}H_{24}$ particle, nevertheless they do not show an oxygen-induced resonance at 2.8 eV. This leads us to believe that the observed band at 440 nm (2.8 eV) is most likely not associated with defects in the

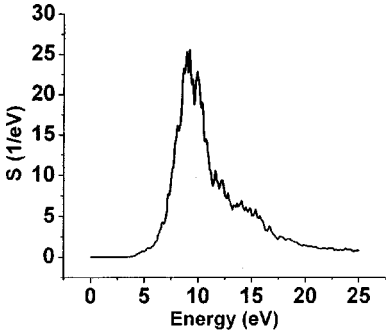

FIG. 6. The absorption spectrum of the $Si_{29}H_{24}^{nano1}$ configuration for the range 0–25 eV, calculated using the same methods as for Fig. 4.

hydrogen passivation such as the presence of a single oxygen site.

Recent quantum Monte Carlo simulations yielded two other variations on the configuration of the $Si_{29}H_{24}$ cluster [Figs. 1(b) and 1(c)].[18] QMC calculation gives band gap edges of 4.5 and 4.1 eV for these two configurations, $Si_{29}H_{24}^{nano1}$ and $Si_{29}H_{24}^{nano2}$. These band edges coincide with the energies calculated for the excited states of the ideal configuration. If we associate the measured resonance excitation energies of 4.0 and 4.5 eV with the band edge E_g, then the measured bands at 3.7, 4.0, and 4.6 eV can be explained if the particle ensemble consists of the three configurations: bulklike, $Si_{29}H_{24}^{nano1}$, and $Si_{29}H_{24}^{nano2}$. The simulations show that these variations in configuration are favorable for several reasons. First, the total energies of the two variations are less than the total energy of the bulklike case by 0.6 and 1.0 eV, respectively. Second, the barrier involved does not require breaking of multiple bonds simultaneously; only a single bond at a time. Third, the two nonbulklike configurations are less strained compared to the bulklike construction.

The band edges of the two configurations $Si_{29}H_{24}^{nano1}$ and $Si_{29}H_{24}^{nano2}$ are found to be close to the energies calculated for the excited states of the bulklike configuration. Thus, it would not be possible based on energy consideration alone to differentiate between the two regimes. There are several potential signatures that may be useful in this regard. These include studies of the excited states in the 4.5–7.0 eV range. There are no other configurations with band gap excitation exceeding 4.5 eV, because this would require restructuring of the bonds in terms of symmetries other than the T_d tetrahedral coordination. In other words, the system would have to switch from the tetrahedral sp^3 symmetry to the graphitelike sp^2 symmetry, which is not favorable in solid silicon. Other means of differentiation include the use of UV light treatment to soften the bonds to determine if the $Si_{29}H_{24}^{nano1}$ and $Si_{29}H_{24}^{nano2}$ configurations can be activated or catalyzed, hence enriching the population of the sample with the different particles. Finally, the theoretical optical properties of the higher excited states of bulklike $Si_{29}H_{24}$ and the $Si_{29}H_{24}^{nano1}$ and $Si_{29}H_{24}^{nano2}$ configurations, including the emission bands, Stokes shifts, brightness, quantum efficiency, optical anisotropy, and vibration spectra, would provide other means of differentiating between the mechanisms.

Using TDDFT and the same parameters (i.e., number of orbitals, cutoffs, etc.) as in the case of the bulklike $Si_{29}H_{24}$ cluster, we calculated the optical response of the two not entirely bulklike configurations. In Figs. 6, 7(a)–7(c), 8, and 9(a)–9(c), the optical responses of $Si_{29}H_{24}^{nano1}$ and $Si_{29}H_{24}^{nano2}$, respectively, are given for various energy ranges. First we observe that the first substantial absorption band for $Si_{29}H_{24}^{nano1}$ occurs around 4.5 eV, while for $Si_{29}H_{24}^{nano2}$ it occurs around 4.0 eV. This would be in fair agreement with QMC predictions if we associate these peaks with the HOMO-LUMO values of 4.5 and 4.1 eV, respectively, given by QMC. However, the TDDFT results show that absorption

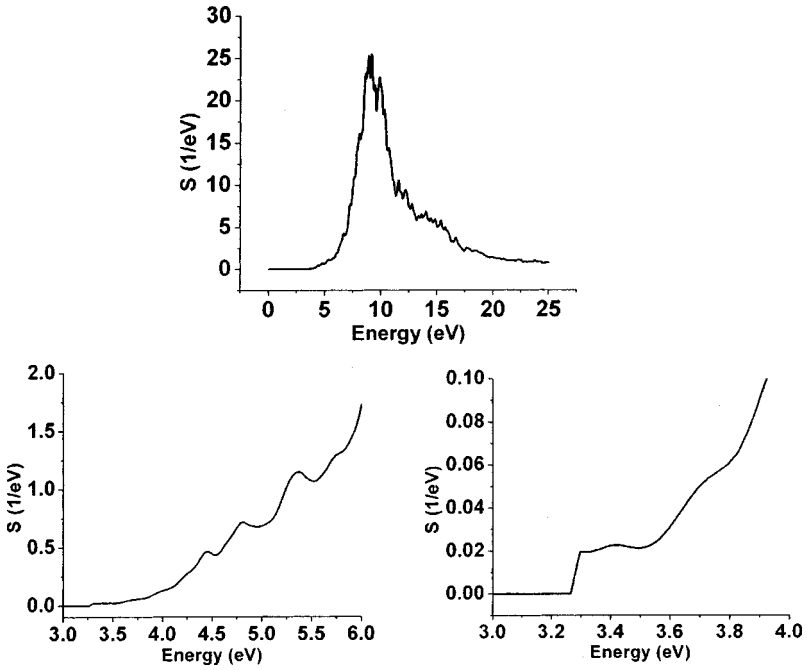

FIG. 7. The absorption spectrum of the $Si_{29}H_{24}^{nano1}$ configuration for different photon energy ranges.

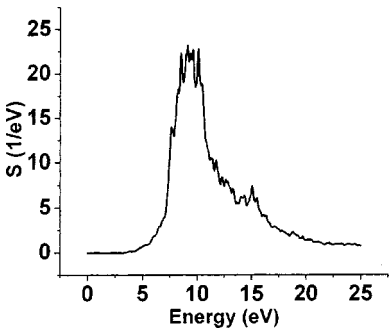

FIG. 8. The absorption spectrum of the $Si_{29}H_{24}^{nano2}$ configuration in the range 0–25 eV, calculated using the same methods as for Fig. 4.

proceeds well below the HOMO-LUMO energies of QMC, down to 3.2 and 3.5 eV, respectively. The second observation is that the low-energy optical response is somewhat different for the two nonbulk configurations. For instance, for $Si_{29}H_{24}^{nano2}$ we see additional peaks at 4.2, 3.85, and 3.5 eV. On the other hand for $Si_{29}H_{24}^{nano1}$, those peaks are nearly washed out. Finally, strong peaks in the TDDFT calculations are in good agreement with the experimental spectra.

The emission and absorption bands of single particles are found to be wide. But they are repeatable with features nearly identical from sample to sample and on any day the material is prepared. Moreover, the measured emission bands of 1, 1.67, 2.15, and 2.85 nm particles are distinct enough to allow reasonable separation according to color, especially the red and blue particles.[6] The importance of size uniformity of silicon clusters, however, transcends issues related to the width of the absorption or emission spectra. For instance, the anisotropy and the time dynamics of photoluminescence have strong dependence on size and shape of the cluster. The fact that transitions in silicon are indirect, therefore requiring phonon-assistance, leads to a dependence of the optical matrix elements on the oscillatory overlaps between electron and hole states in momentum space, which makes the corresponding photoluminescence anisotropy highly sensitive (oscillatory) with the size and shape of clusters.[33] The time dynamics of emission, consisting of multiple time scales, is also sensitive to the size and shape, ranging from nanoseconds for the blue emitting 1 nm to a mix of nanoseconds and hundreds of nanoseconds or microseconds components for the red emitting particles. Moreover, uniformity of size and shape is very important in many photonic or electronic applications that are contemplated for Si nanostructures. For instance, uniformity and repeatability of size and color is important for biomedical applications that employ single molecule analysis using the particles as fluorescent markers, and for synthesis of high quality films, self-assembly formation, or colloidal re-crystallization. In electronics applications utilizing the particles in single electron transistors or charge-based memory nano devices, uniformity is pivotal as size or shape non-uniformity washes out the sharp threshold of the devices.

It is interesting to discuss the Stokes shifts in view of the present results. Figures 5(a)–5(d) show local resonance structure embedded in a continuum of absorption spanning the range 2.6–25 eV. The local resonance is molecularlike with enhanced oscillator strength in absorption. We also believe that it is characterized with enhanced oscillator strength in emission since our measurements show photoluminescence bands commencing at the same resonance energies. For instance, under excitation to the high-lying excited molecularlike state at 280 nm (4.55 eV), the emission bands from the lower excited molecularlike states, peaking at 310, 360, and 400 nm, are observed with decreasing intensity ratios, respectively. Similarly under 310 nm (4.0 eV) excitation, the emission bands from lower excited states, peaking at 360 and 400 nm, are observed. The spacing of the consecutive excited states in the calculated spectrum is inter-

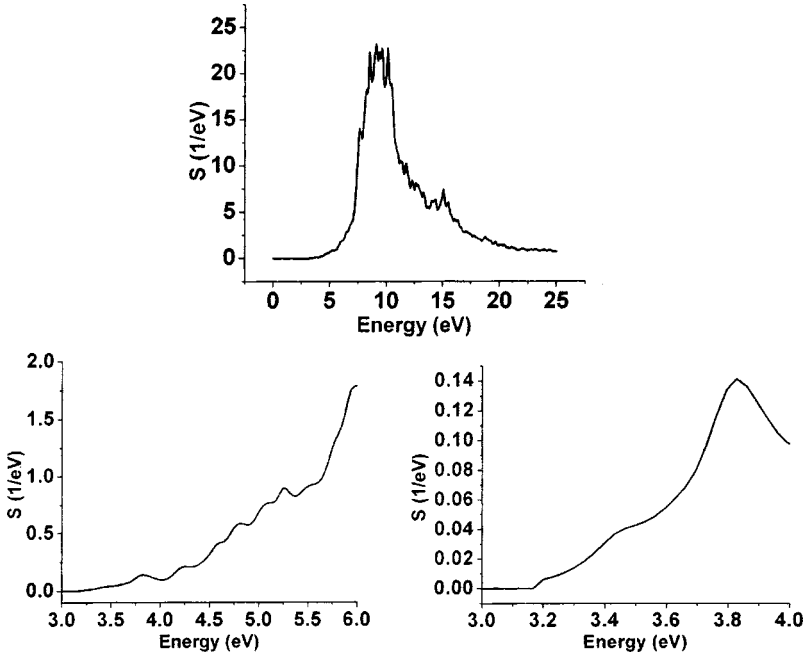

FIG. 9. The absorption spectrum of the $Si_{29}H_{24}^{nano2}$ configuration for different photon energy ranges.

preted as the Stokes shift. The basic mechanism of the cascade process to lower excited states, radiative relaxation via the molecularlike states versus charge carrier relaxation via the underlying continuum states, is not clear at present, however. Studying the optical transitions between the excited states may be useful in elucidating the nature of the cascade. If radiative relaxation is involved, we would expect photoluminescence at ~ 2 μm, corresponding to the Stokes energies (0.6–0.5 eV).

In conclusion, we observed several emission bands in 1 nm Si nanoparticles, a blue band and two UV bands, at 400, 350, and 310 nm with excitation energies at 3.5, 4.0, and 4.6 eV. The measured bands and Stokes shifts are explained in terms of intrinsic molecularlike excited states of the ideal bulklike configuration of the $Si_{29}H_{24}$ nanocluster but some of the bands may originate from similar particles with different surface reconstructions. In order to be able to distinguish between the different structures, and to elucidate the nature of the Stokes shift, extension of the studies to higher energies into the vacuum UV region and monitoring emission or excitation between the excited states in the infrared regime are desirable. Calculations of the optical response can also be useful, as demonstrated with our TDDFT calculations.

ACKNOWLEDGMENTS

The authors would like to thank Dr. E. Draeger for providing the coordinates for the $Si_{29}H_{24}^{nano1}$ and $Si_{29}H_{24}^{nano2}$ clusters. The authors also acknowledge U.S. NSF Grant No. BES-0118053, the State of Illinois IDCCA Grant No. 00-49106, the U.S. DOE Grant No. DEFG02-ER9645439, NIH Grant No. RR03155, and the University of Illinois at Urbana-Champaign.

*Electronic address: m-nayfeh@uiuc.edu

[1] L. T. Canham, Appl. Phys. Lett. **57**, 1046 (1990).
[2] See for example: A. G. Cullis, L. T. Canham, and P. Calcott, J. Appl. Phys. **82**, 909 (1997).
[3] P. Wilcoxson, G. A. Samara, and P. N. Provencio, Phys. Rev. B **60**, 2704 (1999).
[4] M. V. Wolkin, J. Jnes, P. M. Fauchet, G. Allan, and C. Delerue, Phys. Rev. Lett. **82**, 197 (1999).
[5] S. Schuppler, S. L. Friedman, M. A. Marcus, D. L. Adler, Y. H. Xie, F. M. Ross, Y. L. Chabbal, T. D. Harris, L. E. Brus, W. L. Brown, E. E. Chaban, P. F. Szajowski, S. B. Christman, and P. H. Citrin, Phys. Rev. Lett. **72**, 2648 (1994); Phys. Rev. B **52**, 4910 (1995).
[6] G. Belomoin, J. Therrien, A. Smith, S. Rao, R. Twesten, S. Chaieb, L. Wagner, L. Mitas, and M. Nayfeh, Appl. Phys. Lett. **80**, 841 (2002).
[7] O. Akcakir, J. Therrien, G. Belomoin, N. Barry, E. Gratton, and M. Nayfeh, Appl. Phys. Lett. **76**, 1857 (2000).
[8] M. Nayfeh, O. Akcakir, J. Therrien, Z. Yamani, N. Barry, W. Yu, and E. Gratton, Appl. Phys. Lett. **75**, 4112 (1999).
[9] M. H. Nayfeh, N. Barry, J. Therrien, O. Akcakir, E. Gratton, and G. Belomoin, Appl. Phys. Lett. **78**, 1131 (2001).
[10] M. H. Nayfeh, S. Rao, N. Barry, J. Therrien, G. Belomoin, A. Smith, and S. Chaieb, Appl. Phys. Lett. **80**, 121 (2002).
[11] M. H. Nayfeh, O. Akcakir, G. Belomoin, N. Barry, J. Therrien, and E. Gratton, Appl. Phys. Lett. **77**, 4086 (2000).
[12] J. Therrien, G. Belomoin, and M. Nayfeh, Appl. Phys. Lett. **77**, 1668 (2000).
[13] G. Allan, C. Delerue, and M. Lannoo, Phys. Rev. Lett. **76**, 2961 (1996).
[14] M. Nayfeh, N. Rigakis, and Z. Yamani, Phys. Rev. B **56**, 2079 (1997); in *Materials and Devices for Silicon-Based Optoelectronics*, edited by J. E. Cunningham, S. Cotta, A. Polman, and R. Soret, Mater. Res. Soc. Symp. Proc. No. 486 (Materials Research Society, Pittsburgh, 1998), p. 243.
[15] L. Mitas, J. Therrien, G. Belomoin, and M. H. Nayfeh, Appl. Phys. Lett. **78**, 1918 (2001).
[16] L. Wagner, A. Puzder, A. Williamson, Z. Helms, J. Grossman, L. Mitas, G. Galli, and M. Nayfeh (unpublished).
[17] G. Belomoin, E. Rogozhina, J. Therrien, P. V. Braun, L. Abuhassan, M. H. Nayfeh, L. Wagner, and L. Mitas, Phys. Rev. B **65**, 193406 (2002).
[18] E. W. Draeger, J. C. Grossman, A. J. Williamson, and G. Galli, Phys. Rev. Lett. **90**, 167402 (2003).
[19] D. Sundholm, Nano Lett. **3**, 847 (2003).
[20] G. Belomoin, J. Therrien, and M. Nayfeh, Appl. Phys. Lett. **77**, 779 (2000); Zain Yamani, Howard Thompson, Laila AbuHassan, and Munir H. Nayfeh, *ibid.* **70**, 3404 (1997); D. Andsager, J. Hilliard, J. M. Hetrick, L. H. AbuHassan, M. Plisch, and M. H. Nayfeh, J. Appl. Phys. **74**, 4783 (1993); Z. Yamani, S. Ashhab, A. Nayfeh, and M. H. Nayfeh, *ibid.* **83**, 3929 (1998).
[21] D. Sa'nchez-Portal, P. Ordejon, E. Artacho, and J. M. Soler, Int. J. Quantum Chem. **65**, 453 (1997).
[22] E. Artacho, D. Sa'nchez-Portal, P. Ordejon, A. Garcia, and J. M. Soler, Phys. Status Solidi B **215**, 809 (1999).
[23] P. Ordejon, Phys. Status Solidi B **217**, 335 (2000).
[24] N. Troullier and J. L. Martins, Phys. Rev. B **43**, 1993 (1991).
[25] L. Kleinman and D. M. Bylander, Phys. Rev. Lett. **48**, 1425 (1982).
[26] O. F. Sankey and D. J. Niklewski, Phys. Rev. B **40**, 3979 (1989); D. Sánchez-Portal, E. Artacho, and J. M. Soler, J. Phys.: Condens. Matter **8**, 3859 (1996).
[27] R. S. Varga, *Matrix Iterative Analysis* (Prentice-Hall, Englewood Cliffs, NJ, 1962), p. 263.
[28] A. Tsolakidis, D. Sánchez-Portal, and R. M. Martin, Phys. Rev. B **66**, 235416 (2002).
[29] C. S. Garoufalis, A. Zdetsis, and S. Grimme, Phys. Rev. Lett. **87**, 276402 (2001).
[30] Angel Rubio, J. A. Alonso, X. Blase, L. C. Balbás, and Steven G. Louie, Phys. Rev. Lett. **77**, 247 (1996).
[31] I. Vasiliev, J. Chelikowsky, and R. Martin, Phys. Rev. B **65**, 121302 (2002).
[32] Z. Zhou, L. Brus, and R. Friesner, Nano Lett. **3**, 163 (2003).
[33] G. Allan, C. Delurue, and Y. M. Niquet, Phys. Rev. B **63**, 205301 (2001).